

## Article

# Development of a Smart Static Transfer Switch Based on a Triac Semiconductor for AC Power Switching Control

Ahmed H. Okilly <sup>1,2</sup>, Namhun Kim <sup>3</sup>, Jonghyuk Lee <sup>1</sup>, Yegu Kang <sup>1</sup> and Jeihoon Baek <sup>1,\*</sup>

<sup>1</sup> Electrical & Electronics and Communication Engineering Department, Koreatech University, Cheonan 31253, Republic of Korea

<sup>2</sup> Electrical Engineering Department, Faculty of Engineering, Assiut University, Assiut 71516, Egypt

<sup>3</sup> Department of Electrical & Electronics, Korea Polytechnic, Gumi 39257, Republic of Korea

\* Correspondence: jhbaek@koreatech.ac.kr; Tel.: +82-41-560-1258

**Abstract:** Power system disruptions can be categorized as issues with the quality of electricity brought on by voltage sags, lightning strikes, and other system-related interferences. The static transfer switch (STS) has recently emerged as the most important technology for electric power transmission, distribution, and control systems to manage power supply during power system disruption issues, particularly in cost-effectively supplying power to critical loads and sensitive loads without interruption. In this paper, for the switching between the two AC sources during the voltage disruptions issue with low transfer time, a smart static transfer switch (SSTS) based on a digital switching algorithm and Triac semiconductor switch is proposed and experimentally tested. A digital switching algorithm based on online AC voltage sensing and zero-crossing detection is proposed and implemented inside a DSP MCU. The printed circuit board (PCB) of the proposed SSTS is designed and manufactured for the experimental performance investigation with different AC input voltage conditions. A comparative study based on the advantages and disadvantages of the proposed SSTS system with the previous works is also presented. A smart static transfer switch with a transition time of less than one cycle and a digital protection technique during fault conditions is obtained in this work.

**Keywords:** AC power control; smart static transfer switch (SSTS); switching algorithm; zero-crossing detection; transfer time; online AC voltage measurements; Triac



**Citation:** Okilly, A.H.; Kim, N.; Lee, J.; Kang, Y.; Baek, J. Development of a Smart Static Transfer Switch Based on a Triac Semiconductor for AC Power Switching Control. *Energies* **2023**, *16*, 526. <https://doi.org/10.3390/en16010526>

Academic Editor: Salman Mohagheghi

Received: 29 November 2022

Revised: 28 December 2022

Accepted: 30 December 2022

Published: 3 January 2023



**Copyright:** © 2023 by the authors. Licensee MDPI, Basel, Switzerland. This article is an open access article distributed under the terms and conditions of the Creative Commons Attribution (CC BY) license (<https://creativecommons.org/licenses/by/4.0/>).

## 1. Introduction

Nowadays, power quality has gained a lot of importance among residential and industrial customers. Various power quality issues, such as voltage sag, lightning strikes, and service outages affect many industrial loads. Industrial customers suffer significant financial losses as a result of these power quality issues [1,2]. Therefore, in this circumstance, an emergency transfer switch between the preferred and alternative power sources may be the most economical way to avoid these issues [3–5].

Modern industrial facilities contain a variety of sensitive loads that require high-quality electricity to operate steadily and minimize difficulties caused by abrupt voltage interruptions [6,7]. Usually, two main types of switches can be used for handling the source switching process for such sensitive loads—an automatic transfer switch (ATS) [8–10] and a static transfer switch (STS) [11–13].

An ATS is a device that automatically transfers a power supply from its preferred or primary source to an alternative or a backup source when it senses a failure or outage in the primary source. There are two types of automatic transfer switches: a circuit breaker and a contactor. A circuit breaker type has two interlocked circuit breakers, though only one breaker can be closed at any time [14–17]. A contactor type is a simpler design that is electrically operated and mechanically held [18,19].

A static transfer switch (STS), as depicted in Figure 1, can perform the same function as an ATS, but an STS has no mechanical switching devices in which the semiconductor devices, such as thyristors [20–23], gate turn off (GTO) thyristors [24–26], insulated gate bipolar transistors (IGCTs) [27–29], insulated-gate bipolar transistors (IGBTs) [30] or Triac [31,32] semiconductor devices, can be used for the switching process. A comprehensive overview and a comparative study between the different semiconductor devices utilized in AC power switching control were performed, as shown in Table 1, according to the different performances such as conduction losses, on-state voltage drop, switching speed, operating frequency, and specific applications.

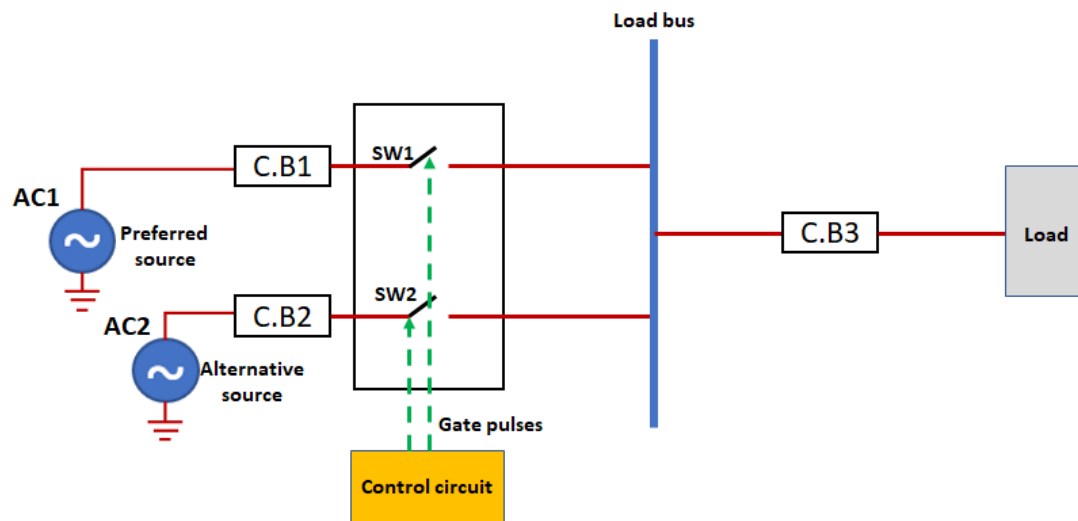


Figure 1. Basic configuration of the AC source switching-based static transfer switch.

Table 1. Comparison of the different semiconductor devices' performances.

Performance	Thyristor (SCR)	GTO	IGCT	IGBT	Triac
Production year	1956	1962	1996	1983	1958
Current flow	Unidirectional	Unidirectional	Unidirectional	Unidirectional	Bidirectional
Voltage-withstanding capability	Bipolar	Bipolar	Unipolar	Unipolar	Unipolar
On-state voltage	High	Very high	High	Low	Low
Operating frequency	Low	Low	Low	High	Low
Conduction losses	High	Very high	High	Low	Low
Drive circuit	Very simple	Complex	Simple	Very simple	Simple
Switching speed	Medium	Fast	Fast	Very fast	Very fast
Cost	Low	High	High	High	Low
Specific applications	AC power control, HVDC systems, oscillators, and inverters	AC power control, variable-speed drives, high-power traction systems, and inverters	Variable-frequency inverters and fast AC disconnect switches	AC and DC motor drives, SMPS, and UPS	AC power control and motor speed control

For AC power switching control at low and medium voltage levels, a conventional circuit of an STS is usually implemented with the use of thyristor or GTO semiconductor

switches, and a thyristor-based STS has many advantages such as low costs, low conduction loss, and simple gate driver circuit implementation as compared to STS-based GTO and IGCT switches for the same operating conditions [24,33,34]. For switching control at medium voltage levels, an STS-based IGBT can present excellent performance elements such as low conduction losses and fast switching speed with simple gate driver circuit implantation [30]. For high voltage and extra high voltage levels, solid-state wide bandgap semiconductor devices, such as silicon carbides (SiC), static induction transistors (SITs), SiC metal oxide semiconductor field effect transistors (MOSFETs), and SiC junction gate field effect transistors (JFETs), are rapidly advancing in technology. These devices can provide a superior switching performance and are far superior to their mechanical counterparts in addressing power quality issues [35,36].

Recently, the Triac has been the most commonly used semiconductor device for switching and power control of AC systems as a Triac can be switched on by either a positive or negative gate pulse, regardless of the polarity of the AC supply at that time. In addition, in AC power switching control, when using a Triac semiconductor device (a bidirectional device), it only requires one heat sink, but the other unidirectional devices require two heat sinks. A Triac also requires only one fuse for protection, and while a safe breakdown can occur in either direction, unidirectional devices should have parallel diode protection.

One of the advantages of an STS-based Triac semiconductor is that it is typically utilized with the ability to transfer the critical load at the point of zero-crossing in an AC waveform where there is no net flow of power to the load, which offers the best opportunity to undertake a change-over with high reliability [34,37]. In this instance, the zero-crossing switching technique can help to prevent an inrush current due to the high  $dv/dt$  from flowing through the system's different components, which provides more protection [38–40]. However, in case of a loss of the primary source, the transfer is completed at any point in the waveform to avoid a break in supply to the sensitive loads [41–43]. Furthermore, an STS is typically implemented to offer operation with an interruption or transfer time of less than one cycle, which is small compared to the transfer time in the case of an ATS [44–47]. The selected semiconductors used in the implementation of an STS should be rated with large safety margins to ensure long life and reliable operation [37,48].

In this study, the overall structure of a smart static transfer switching system based on Triac switches and a digital control algorithm is proposed. The AC voltage measurement circuit is designed for online AC voltage sensing and interfacing with a DSP MCU, and the control technique inside the DSP is proposed based on the digital switching algorithm, with zero-crossing detection for the switching operation of the Triac switches and interrupt service routine (ISR) for system protection during the fault condition. The power and control circuits of the proposed SSTS system are designed and manufactured in a printed circuit board (PCB) for the experimental verification of the designed SSTS system's performance with different operating conditions.

This paper is organized as follows: In Section 2, we describe the overall configuration and basic control method of the proposed SSTS-based DSP MCU and Triac switches. In Section 3, we briefly describe the proposed switching algorithm, the zero-crossing detection technique, and the designed online voltage measurement circuit. The experimental verification by developing the printed circuit board (PCB) of the smart static transfer switching using Triac switches and the digital control circuit using a DSP TMS320 F28035 is provided in Section 4. Section 5 presents a comparative study of the advantages and disadvantages of the proposed switching technique and previous work. Finally, our conclusions are presented in Section 6.

## 2. Overall Structure of the Proposed SSTS Switching System

The basic structure of the proposed two-source switching circuit with an SSTS, as shown in Figure 2, can be summarized as follows:

- A load which is usually sensitive to variations in utility supply voltage in such circuit topologies
- Two independent sources, one of which is the preferred one (AC1) and the other being the alternate one (AC2)
- Two semiconductor switches (Triac1 and Triac2) which connect the load to the two power sources
- The thermal circuit breakers, C.B 1 and C.B 2, are used to protect the components and equipment from current overload and short circuit conditions (or they can be replaced by a current fuse)
- The noise and harmonic filters, used to reject the AC sources' harmonics and reduce the electromagnetic interface (EMI) levels, are connected to the load side
- The controlling algorithm implemented inside the DSP MCU to monitor the AC voltage of both sources, detect normal and abnormal conditions in both supplies, and perform a load transfer from one source to the other, if needed, by controlling the gate pulses of the Triac switches, as well as to protect the system under fault conditions, was implemented using an interrupt service routine (ISR), which shuts down both Triac switches during fault detection

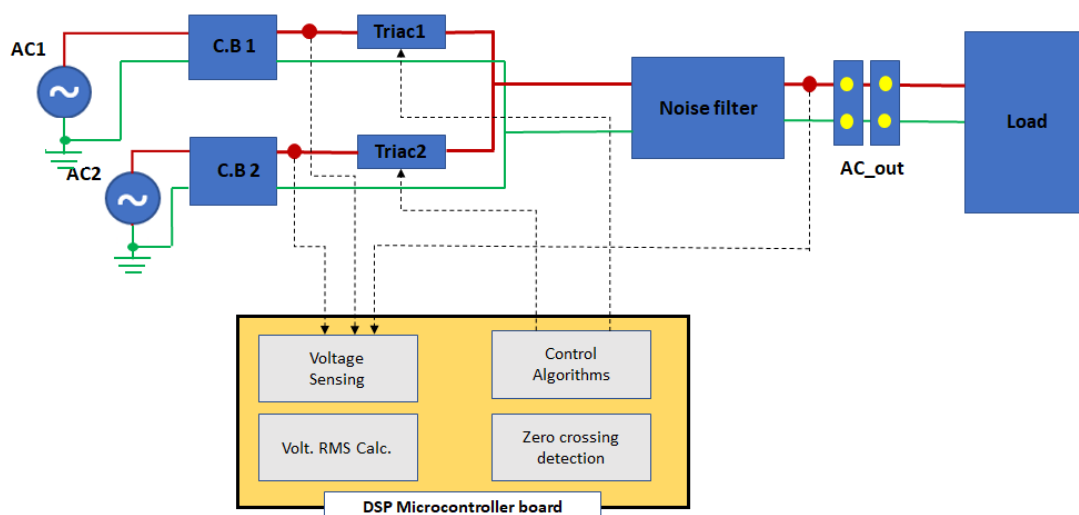


**Figure 2.** Overall configuration of the proposed two-source switching circuit with an SSTS.

### *Principle Operation of the SSTS*

Under normal operating conditions, i.e., when the source AC1 meets load voltage requirements, the control logic triggers only Triac1. If AC1 cannot meet the voltage requirements, the control logic will transfer the load to source AC2 if it is in a better condition. This is achieved by removing the gating signals from Triac1 and triggering Triac2. To offer ride-through capability, the load must be transferred within a very small transfer time. Therefore, the SSTS must meet the following requirements:

- It must detect voltage fluctuations in the system as fast as possible.
- In case the preferred source fails, it must perform a fast load transfer to the alternate source.
- The gating strategy, which controls the transfer process, must prevent the two sources from paralleling.
- Voltage sensing and switching processes between both sources must function properly for all possible operating conditions.

The switching between the two sources (AC1 and AC2) is performed based on the voltage conditions of both sources. The normal condition of the voltage supply to the load from any source is considered to be in the range of  $220\text{ V} \pm 20\% \text{ V}_{\text{rms}}$ . Table 2 shows the

possible operating conditions of the two AC sources and the turn-on sequence of the Triac switches.

**Table 2.** The turn-on sequence of the Triac switches.

AC Source 1	AC Source 2	On Sequence
Normal	Normal	Triac1
Normal	Abnormal	Triac1
Abnormal	Normal	Triac2
Abnormal	Abnormal	Fault

### 3. The Proposed Digital Switching Algorithm

Figure 3 depicts the flowchart of the proposed switching algorithm with the interrupt service routine (ISR) for the proposed SSTS system. The proposed algorithm consists of three parts. The first part is implemented as the ready mode, which contains the system's different parameters' initial values, the Triac switches' initial switching conditions (Triac1 is on and Triac2 is off), and the analog–digital converter (ADC) offset check. The second part is the run mode, which starts with AC1 and AC2 voltage sensing to decide the switching-on/-off condition for Triac1 and Triac2 based on the voltage condition of both sources, according to the turn-on sequence shown in Table 2. To reduce the inrush current due to the high  $dv/dt$  to flow through the Triac switches and to prevent the load power interruption during the transfer process from any source to another, the gate pulses of the Triac switches are offered at the second-next zero-voltage crossing point, followed by the point of the fault detection in which the load net-power flow is exactly equal to zero at that point. The third part (fault mode) of the switching algorithm is implemented to protect the load at the fault condition where both sources are at abnormal conditions by switching off both Triac switches.

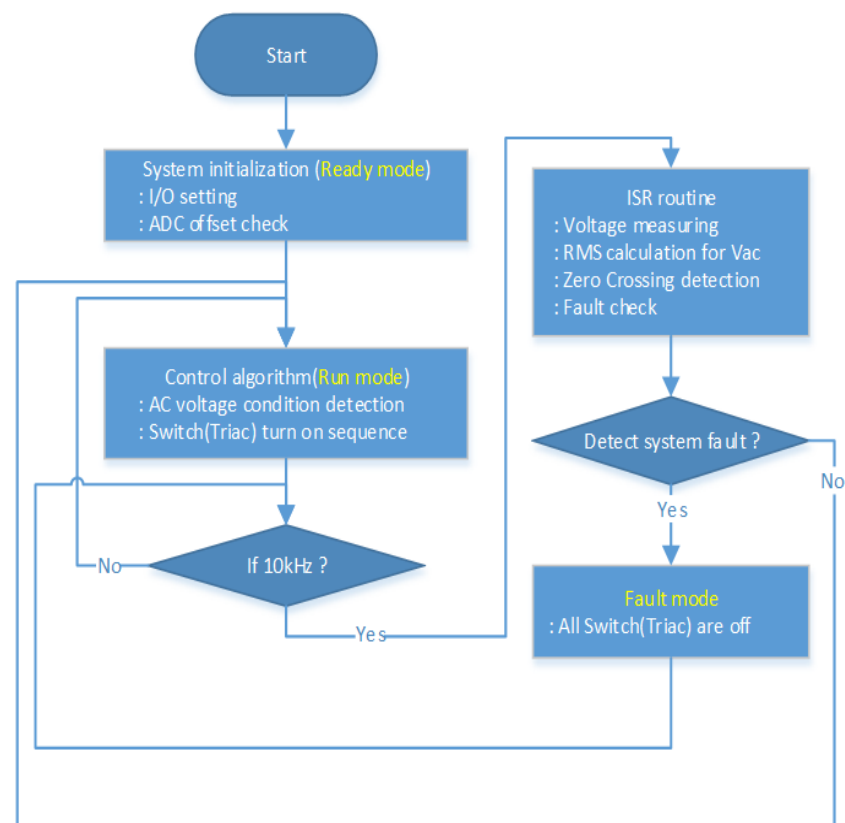


**Figure 3.** Flowchart of the proposed digital switching algorithm.

To select an optimal DSP MCU board to implement the proposed static transfer switching system with the proposed switching algorithms and for the exact zero-crossing point detection, there are important DSP MCU selection considerations, which can be summarized as follows: a program memory large enough to process the data and a data memory large enough to store the information during the voltage signal monitoring and zero-crossing signal detection; an efficient computing engine for performing the math processing and accessing the program from the program memory and the data from the data memory; and an ADC with enough resolution and enough bits for the proper detection the zero-crossing point.

Considering these selection considerations, in this work, the TMS320 F28035 from Texas Instruments with a 32-bit, 60 MHz, 128 KB flash memory and an ADC resolution of 12 bits is selected to implement the control circuit of the proposed switching schemes. The selected DSP is featured with a fast interrupt response and an excellent performance for storage and processing the data, which enable exact zero-crossing point detection with high reliability.

### 3.1. The Proposed Online AC Voltage Measurement Circuit

Figure 4 shows the AC voltage-sensing circuit. In order to realize the function of electrical isolation between the main circuit and the control circuit of the power supply, an isolated optocoupler called HCPL-7840 is used to sense the ac voltage signals from sources one and two.

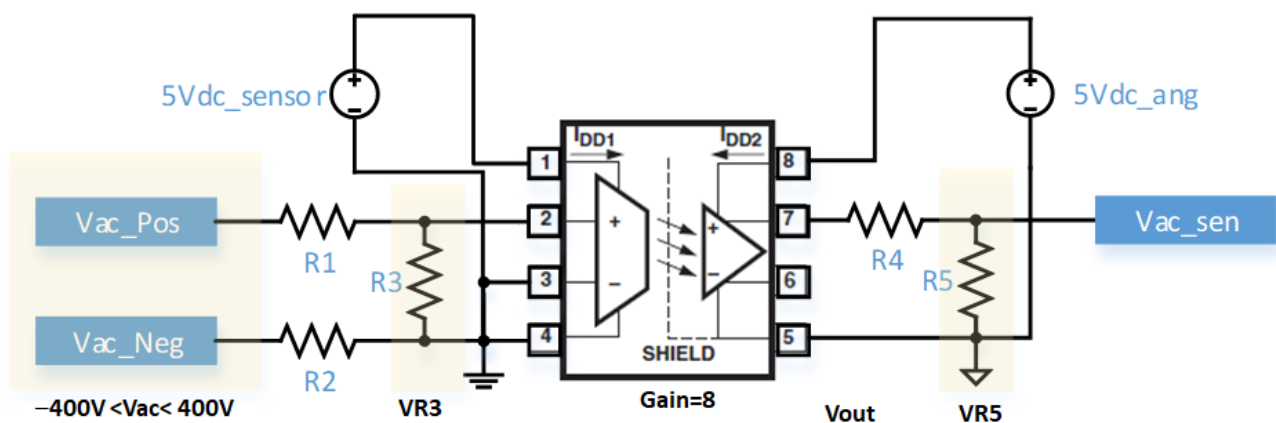


**Figure 4.** Schematic of the designed online AC voltage measurements circuit.

An HCPL7840 is typically designed for current-sensing in electronic motor drives. In a typical implementation, a motor's currents flow through an external resistor and the resulting analog voltage drop is sensed by the HCPL-7840. A differential output voltage is created on the other side of the HCPL-7840 optical isolation barrier. An HCPL-7840 has a very small input offset voltage—less than 0.3 mV—and a high bandwidth of approximately 100 kHz, with a very small nonlinearity ratio of approximately 0.004%, which makes it perfect for the AC voltage signals related to circuit protection and operation management in this application.

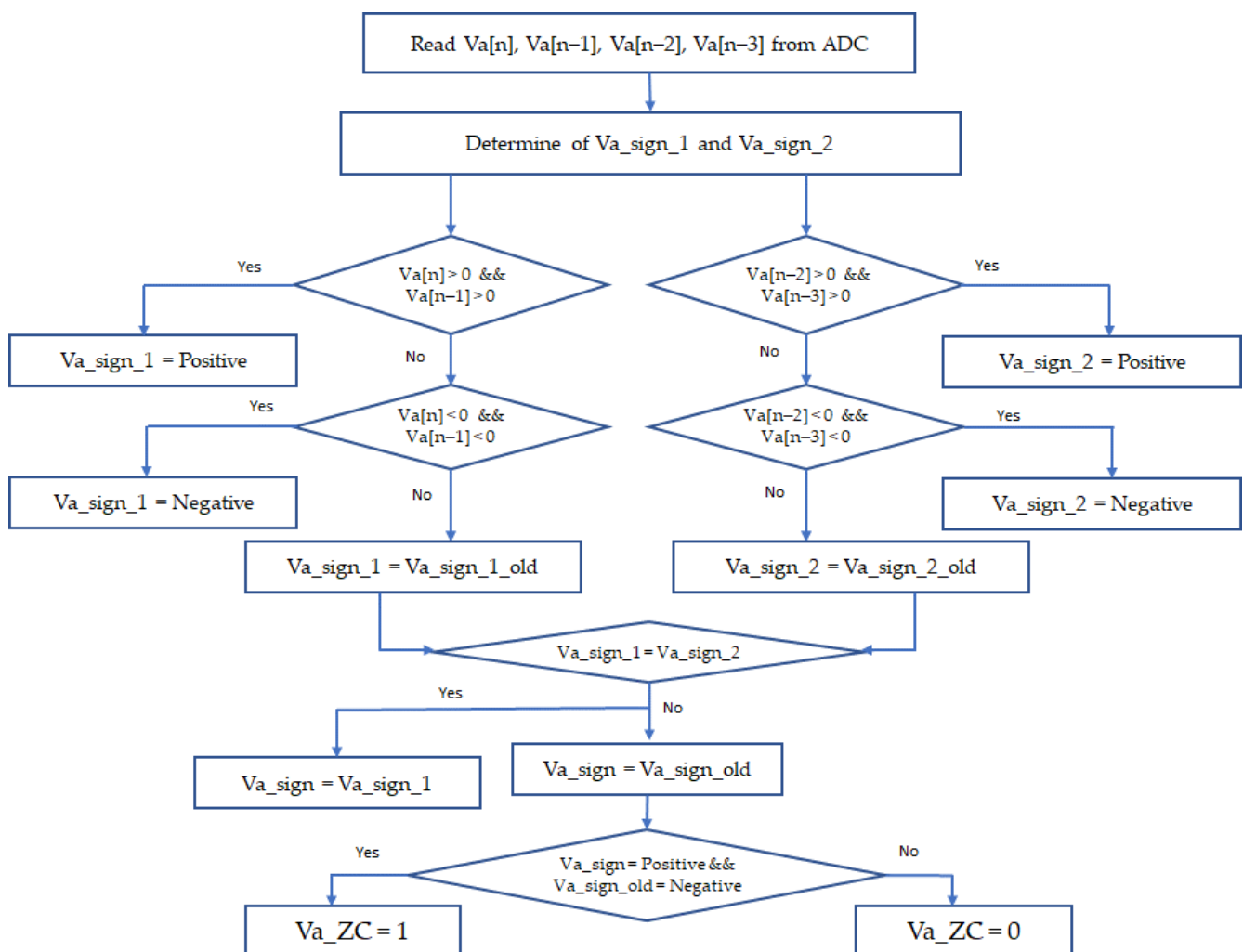
In this work, the proposed AC voltage sensors based on the isolated optocoupler circuit are designed to measure AC voltage with maximum values of  $-400\text{ V}$  to  $+400\text{ V}$ . The input side resistors  $R1$ ,  $R2$ , and  $R3$  are designed to maintain the input voltage ( $VR3$ ) to the HCPL-7840 at the standard limit provided in the datasheet ( $-0.2\text{ V}$  to  $0.2\text{ V}$ ), and with these input voltage conditions and the gain of the used isolated optocoupler IC, which is approximately 8, the output voltage ( $Vout$ ) is in the range of  $0.94\text{ V}$  to approximately  $4.14\text{ V}$ . Therefore, the other resistors ( $R4$  and  $R5$ ) are used to maintain the output voltage in the voltage range of the used analog–digital converter (ADC) of the TMS320 F28035 DSP board.

### 3.2. The Proposed Zero-Voltage Crossing Detection Technique

The instant at which there is no voltage is known as zero-crossing. This often happens twice during each cycle of a sine wave or other straightforward waveforms. When the voltage is zero, and making or breaking connections is the simplest task [41]. A larger inrush current would result from turning on the Triac when the voltage is almost at its peak, which could harm the semiconductor device or result in unwanted electrical noise [41,44]. The safest method is to turn it on while the voltage is zero.

In this work, a zero-voltage detection digital technique is proposed to control the turn-on sequence of the Triac switches after the voltage disturbance occurs at any AC supply, where the Triac switches are switched at the second-next zero-crossing point after the abnormal detection point.

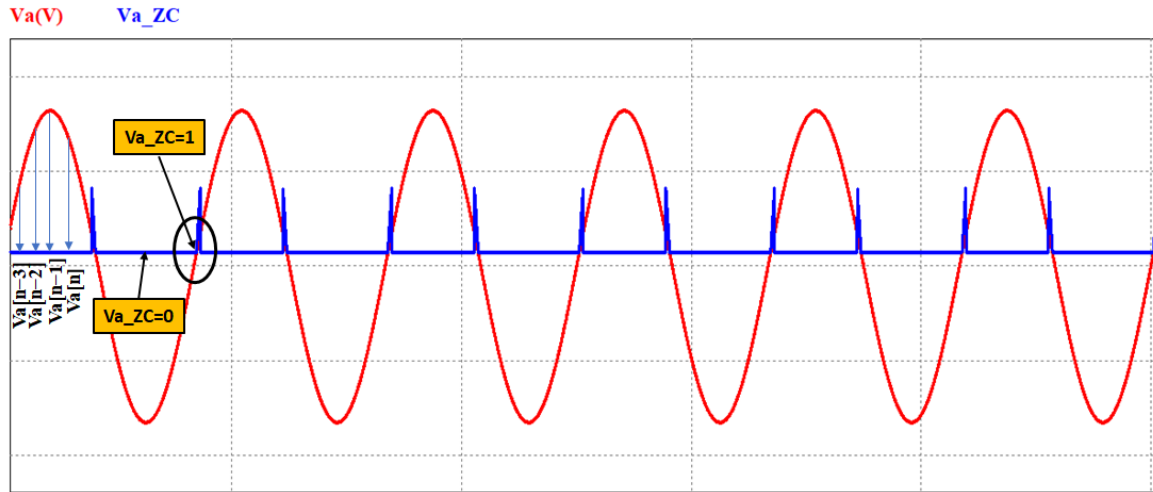
Figure 5 shows a flowchart which describes the proposed technique implemented inside the DSP MCU to detect the zero-voltage crossing point for any AC voltage signal ( $V_a$ ), where, the  $V_a[n]$  is related to the presently measured voltage signal,  $V_{a\_sign\_1}$  is the polarity of the first-measured voltage signal,  $V_{a\_sign\_2}$  is the polarity of the next-measured voltage signal, and  $V_{a\_sign\_old}$  is the polarity of the previous one.



**Figure 5.** Flowchart of the proposed zero-crossing detection technique.

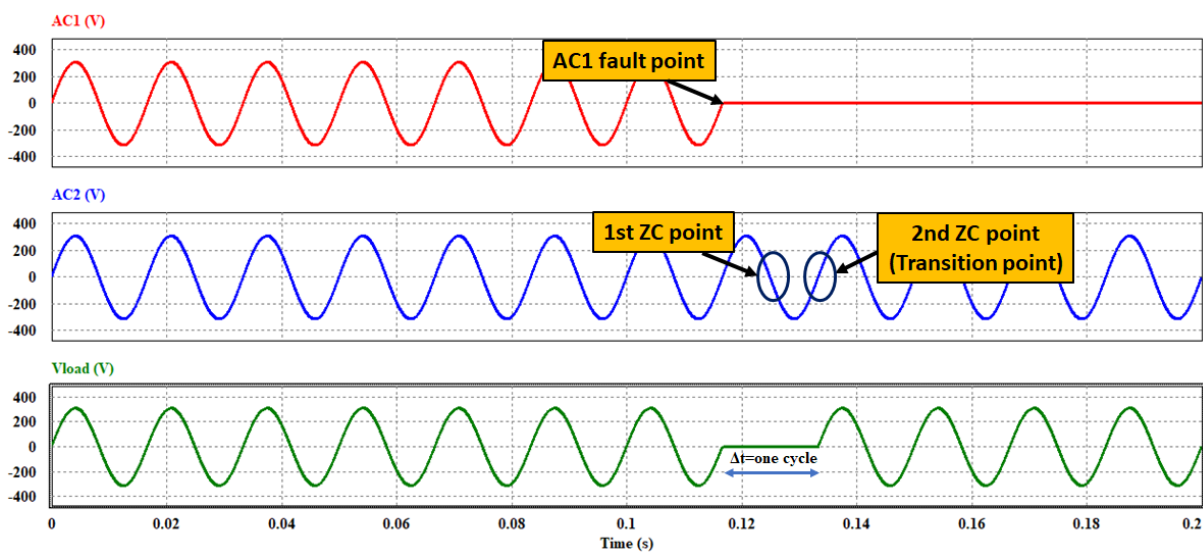
Figure 6 shows the generated zero-voltage crossing signals ( $V_{a\_ZC}$ ) for any pure sine wave voltage signal ( $V_a$ ) using PSIM software. The Triac switches in the proposed SSTS system are controlled to be turned on at the second-next point of the zero-voltage crossing point ( $V_{a\_ZC} = 1$ ) after detecting the abnormal voltage condition of the AC sources. In the

calculation of the proposed switching algorithm, four sampling delay signals are considered; therefore, to obtain precious voltage information and zero-crossing detection, the sampling frequency for the ISR routine is selected with a high enough value (approximately 10 kHz).



**Figure 6.** Zero-voltage crossing detection signal generation ( $V_{a\_ZC}$ ) of any AC voltage pure sine waveform ( $V_a$ ).

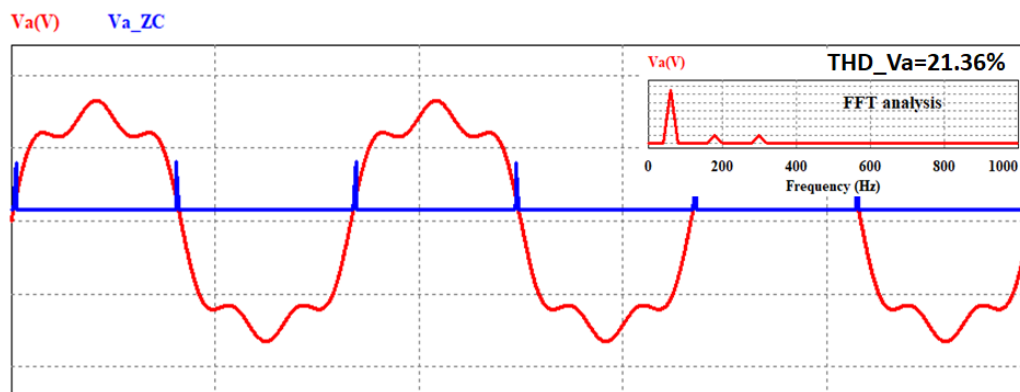
In applying the proposed switching algorithm with the ability of the zero-crossing switching to the used Triac switches, the transition time of the designed SSTS system between the two sources with any operating conditions and when AC1 or AC2 is faulted at any point of the waveform (zero-crossing, fall time, or rise time), the transition time will be within the one cycle. For clear observation, Figure 7 shows the waveforms of the supplies (AC1 and AC2) and the load voltages at the worst case (longest transition time) in which AC1 (or AC2) is faulted at the zero-crossing point. In this case, it is noticed that the proposed SSTS system has a transition time of approximately one cycle only, in which Triac 1 is switched off and Triac 2 is switched on at the second zero-crossing point after the AC1 fault occurrence.



**Figure 7.** Supply and load voltage waveforms and the transition point of the proposed SSTS when the AC1 and AC2 sources are pure sine waves and the AC1 source is faulted at the zero-crossing point (worst case).

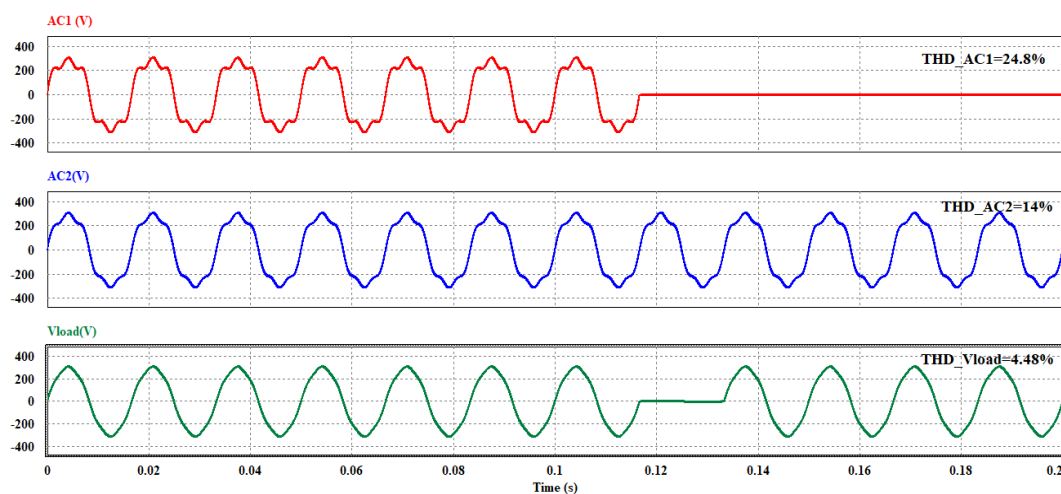
In order to investigate the behavior of the proposed switching algorithm when the voltage is affected by the power quality disturbances (a non-pure sine wave input AC voltage), the zero-crossing detection technique and the whole switching algorithm are tested with the injection of the third and fifth harmonics to the input supplies (AC1 and AC2).

Figure 8 shows the generated zero-voltage crossing signals ( $V_{a\_ZC}$ ) for the non-pure sine wave voltage signal ( $V_a$ ) with a THD value of approximately 21.36%. It contains the third and fifth harmonics components, as shown in the FFT analysis in the same figure, and it is clearly observed that the proposed zero-crossing detection technique is successful in detecting the zero-crossing points of the waveforms, which did not affected by the power quality disturbance of the supply voltage.



**Figure 8.** Zero-voltage crossing detection signal generation ( $V_{a\_ZC}$ ) of a non-pure sine voltage waveform ( $V_a$ ).

In addition, to test the proposed switching algorithm when AC1 and AC2 are affected by the power quality disturbance, Figure 9 shows the voltage waveforms when the AC1 and AC2 voltages are non-pure sine waves and the AC1 source is faulted at the zero-crossing point. This shows that when the fault occurs, the switching system turns off Triac1 and turns on Triac2 at the second zero-crossing point, unaffected by the sources' power quality disturbances. Furthermore, the connected load filters reduce the THD value of the load voltage side to approximately 4.48%.



**Figure 9.** Supply and load voltage waveforms and the transition point of the proposed SSTS when the AC1 and AC2 sources are non-pure sine waves and the AC1 source is faulted at the zero-crossing point (worst case).

### 4. Experimental Verification

Figure 10 shows the schematic circuit of the designed SSTS circuit, where the V.S. circuits represent the proposed AC voltage sensors presented in Figure 4, and for the circuit component protection at the overcurrent condition, the 220 V RMS fuse is used with a current rating equal to the rated load current. The proposed switching algorithm with zero-crossing detection and ISR techniques is implemented using a TMS320 F28035 DSP MCU from Texas Instruments. Under the resistive loading condition of approximately 3 Kohm and using a TELEDYNE scope, the voltage waveforms performances of both AC sources and the load are investigated with the different operating conditions provided in Table 2. To reduce the harmonics and EMI levels on the load side, a WT-RC30-SF noise filter from World Tech company is connected in parallel with the load terminals. Figure 11 shows the designed printed circuit board (PCB) and the overall experimental testing setup of the proposed SSTS switching system for the two synchronized AC power sources with nominal voltages of 220 V RMS and 60 Hz.

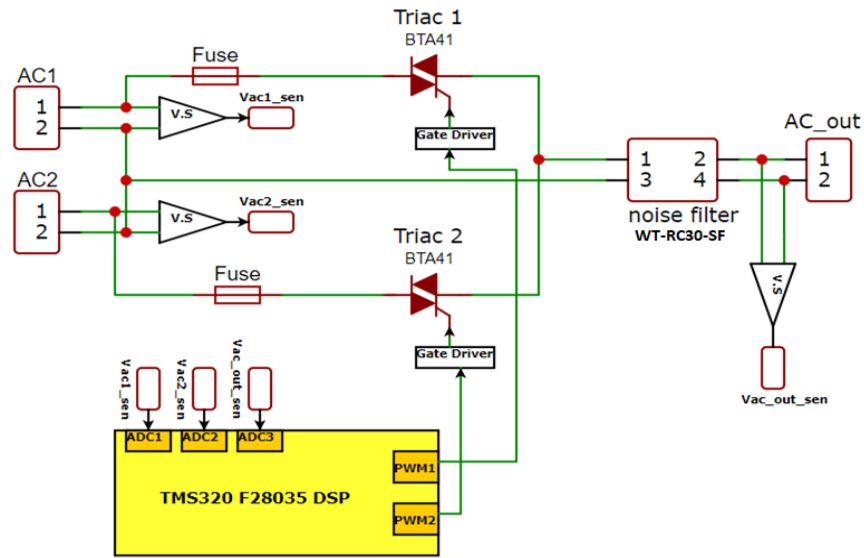


Figure 10. Schematic circuit of the proposed SSTS board for experimental testing (where V.S represents the proposed online voltage sensing circuit presented in Figure 4).

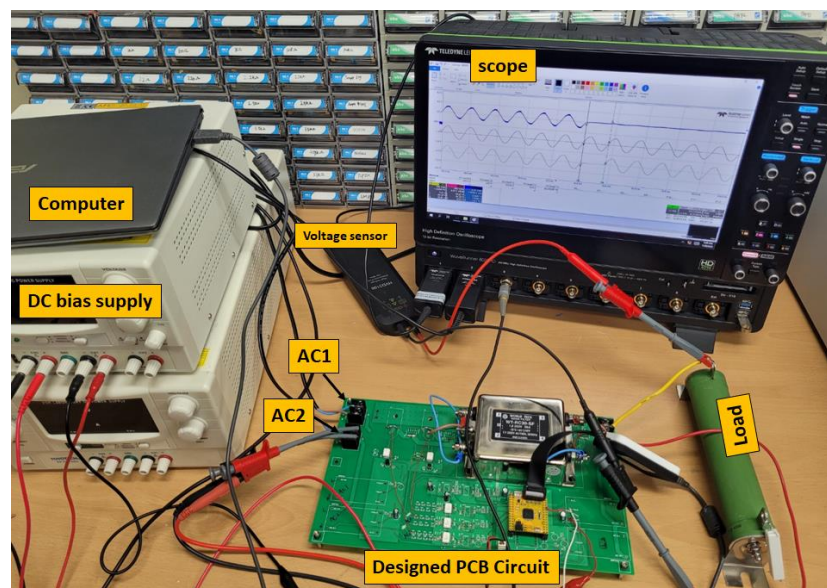
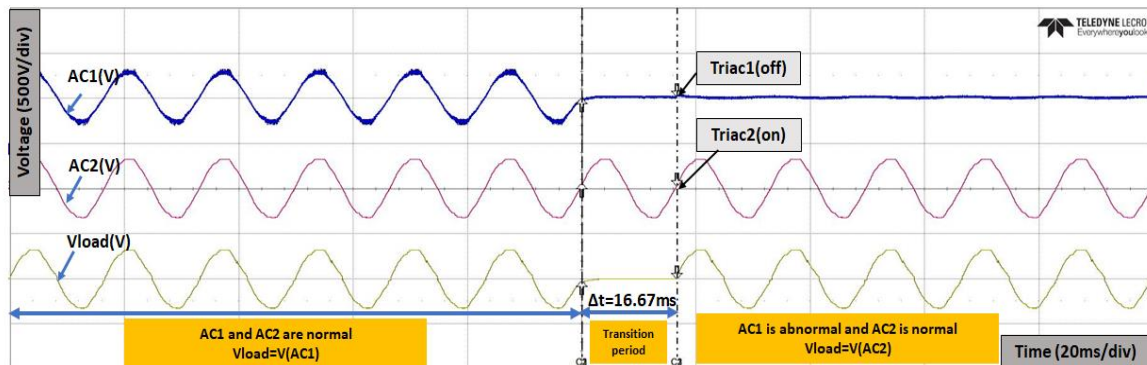


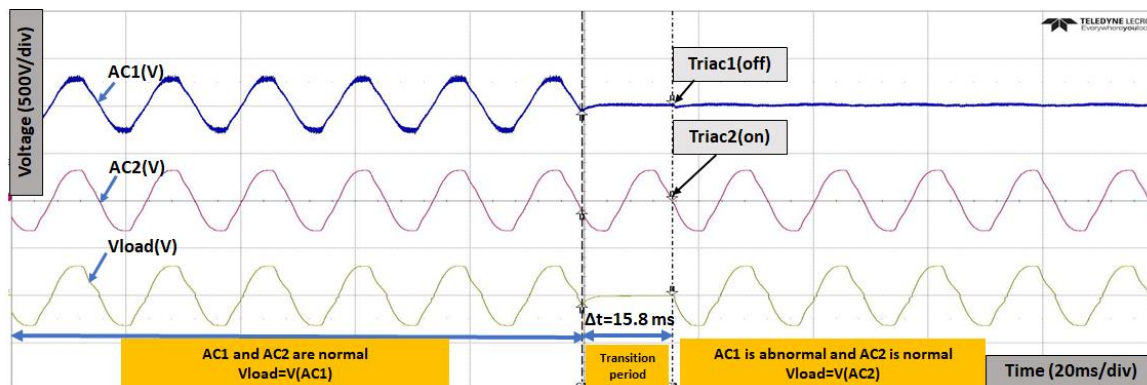
Figure 11. The experimental testing setup of the proposed SSTS switching system.

Figure 12 shows AC1, AC2, and the load voltage waveforms when the AC1 source is faulted precisely at the point of the zero-crossing (worst case). It is observed that the period when AC1 and AC2 are in normal conditions, Triac1 is switched on, Triac2 is switched off, and the load voltage is equal to the AC1 source voltage. When the fault occurs at the AC1 source, the proposed control algorithm will detect the fault and transfer the power supply from AC1 to AC2 at the second-next voltage zero-crossing point with a transition time of approximately 16.67 ms, which is approximately one cycle.



**Figure 12.** Experimental voltage waveforms and transition time calculations when the AC1 source is faulted at the point of zero-crossing.

Figure 13 shows the voltage waveforms and the transition time calculations when the AC1 source is faulted during the voltage waveform fall time. It is noticed that the proposed control algorithm will detect the fault and transfer the power supply from AC1 to AC2 at the second-next voltage zero-crossing point, with a transition time of approximately 15.8 ms (less than one cycle).



**Figure 13.** Experimental voltage waveforms and transition time calculations when the AC1 source is faulted during the voltage waveform fall time.

Figure 14 shows the voltage waveforms and the transition time calculations when the AC1 source is faulted during the voltage waveform rise time. It is noticed that again, the proposed control algorithm will detect the fault and transfer the power supply from AC1 to AC2 at the second-next voltage zero-crossing point, with a transition time of approximately 14 ms (less than one cycle).

From Figures 12–14, it is clearly observed that when the AC1 fault condition occurs at any point of the voltage waveforms, the proposed SSTS system successfully detects the fault and transfers the power supply from the AC1 source to the AC2 source with a transition time of less than one cycle.

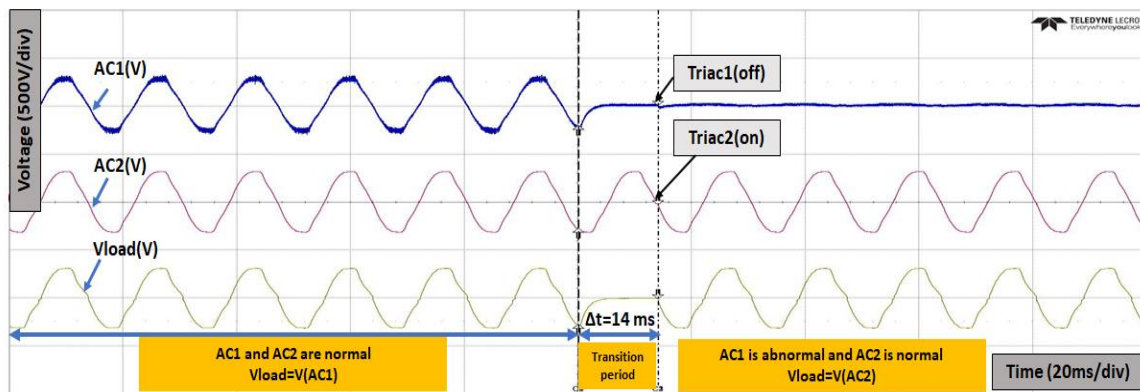


**Figure 14.** Experimental voltage waveforms and transition time calculations when the AC1 source is faulted during the voltage waveform rise time.

The operation principle of the proposed SSTS system is similar when the AC1 source is faulted instead of the AC2 source. To verify these operation conditions, Triac1 is switched off and Triac2 is switched on, and then the AC2 source is faulted at the zero-crossing point, and by applying the proposed switching algorithm, as shown in Figure 15, it is noticed that when the fault occurs at the AC2 source, the proposed control algorithm will detect the fault and transfer the power supply from AC2 to AC1 at the second-next voltage zero-crossing point, with a transition time of approximately 16.22 ms.

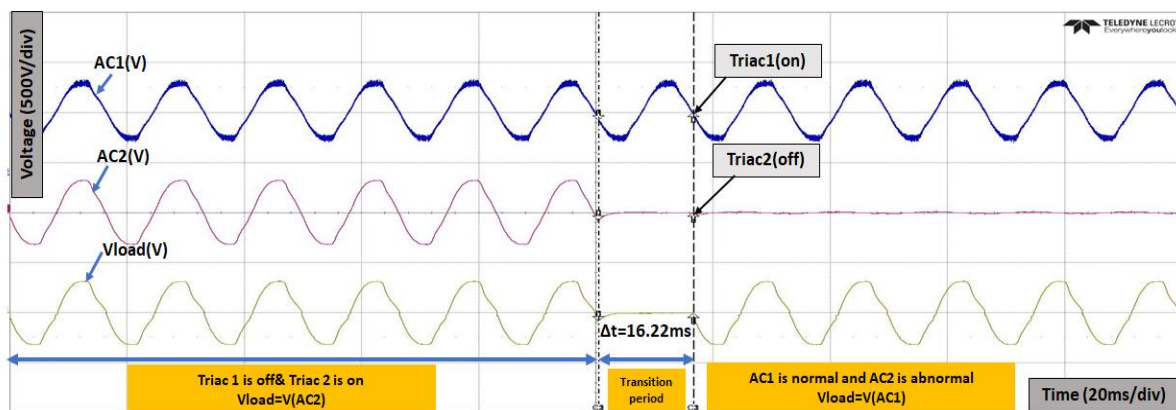


**Figure 15.** Experimental voltage waveforms and transition time calculations when the AC2 source is faulted at the point of zero-crossing.

## 5. Comparison of the Proposed SSTS System with Previous Works

Table 3 shows the advantages and disadvantages of the proposed switching system with previous works that used different semiconductor devices and control techniques and different testing platforms.

**Table 3.** Performance comparison of the proposed SSTS with previous works.

Ref.	Configuration	Testing Platform	Control Techniques	Disadvantages	Advantages
Proposed	STS-based Triac	Experimental	Voltage monitoring, zero-crossing detection, and ISR implementation	Fault detection based on voltage monitoring only and there is no current sensing	Simple construction, exact zero-crossing detection, load protection, reduced inrush current, and short transition time within one cycle
[21]	STS-based thyristor	PSCAD/EMTDC simulation	Voltage sag detection based on synchronous reference frame	Fault detection based on voltage monitoring, but without current sensing, complex commutation circuits, and zero-crossing detection	Short transition time (within one cycle), preventing the source from paralleling and preventing the flow of the cross-current
[22]	Hybrid ATS plus STS based-thyristor	Experimental	Voltage monitoring and BBM technique to decide exact transfer point	High transfer time (more than one cycle), high cost, and complex power and control circuit configuration	Reduced power losses and reliable for applications with high voltage and power capacity
[20]	STS-based thyristor	Experimental	Voltage monitoring and machine learning technique	No current sensing, complex control algorithms, and zero-crossing detection	High accuracy and short transition time
[23]	STS-based thyristor	PSCAD/EMTDC simulation	Voltage monitoring based on PLL and BBM techniques	No zero-crossing detection	Fast synchronization and short transfer time with the PLL and BBM techniques
[27]	STS-based IGCT	Experimental	Voltage source converter and DC chopper circuit	Using the dissipation resistors in the circuit construction increased the circuit size and thermal losses	High reliability with low cost for very-high-power applications
[13]	STS-based thyristor	MATLAB simulation	Voltage and current signal detection using the dq transformation	No zero-crossing detection	Voltage and current sensing to detect the power disturbance and a short transition time

## 6. Conclusions

A smart static transfer switch (SSTS) based on a Triac semiconductor switch and digital control switching algorithm is proposed in this paper. The SSTS system is designed to control the power transfer from the preferred power supply to an alternate power supply with a transition time of less than one cycle. The zero-crossing switching technique is offered in the proposed switching algorithm for the Triac switches during the transition process, helping to reduce the inrush current due to the high  $dv/dt$ . Furthermore, an interrupt service routine (ISR) is implemented to protect the loads during the fault conditions when all available sources are at abnormal conditions. The printed circuit board (PCB) of the proposed SSTS was designed and manufactured, and the experimental results show that when the fault occurs at the AC power source connected to the load, the proposed switching algorithm successfully senses the AC voltage, detects the fault condition, predicts the zero-crossing point, and converts the power from the preferred source to the alternate source with a transition time of within one cycle (at the worst case).

For future work related to this research, the switching algorithm based on the online measurements and monitoring of the voltage and current waveforms (and not only the

voltage waveforms) should be conducted to increase the circuit reliability and protect the circuit components during the overload conditions. In addition, the design and coordination of the communication and SCADA system to remotely operate the semiconductor switches will also be completed. Furthermore, the design and the experimental performance investigation of the SSTS will be extended to work with three-phase AC systems with the same and different voltage sequences.

**Author Contributions:** Design and application—the literature review and manuscript preparation, as well as the simulations, were carried out by A.H.O. and N.K. The experimental results and implementation of the prototype were carried out by J.L., N.K. and Y.K. Final review of the manuscript and corrections were completed by J.B. All authors have read and agreed to the published version of the manuscript.

**Funding:** This research was funded by a grant (RS-2022-00142883) from the Ministry of Land, Infrastructure and Transport of the Korean government. In addition, this work was supported by the “Leaders in Industry-university Cooperation 3.0” project grant (1345356194) funded by the Ministry of Education and National Research Foundation of Korea.

**Data Availability Statement:** Not applicable.

**Conflicts of Interest:** The authors declare no conflict of interest.

## References

1. Souza, M.E., Jr.; Freitas, L.C. Power Electronics for Modern Sustainable Power Systems: Distributed Generation, Microgrids and Smart Grids—A Review. *Sustainability* **2022**, *14*, 3597. [[CrossRef](#)]
2. Jung, J.H.; Kim, H.S.; Lee, J.; Nho, E.C. Voltage disturbance generator output characteristics for the test of microgrid with STS. In Proceedings of the 2017 IEEE 3rd International Future Energy Electronics Conference and ECCE Asia (IFEEC 2017-ECCE Asia), Kaohsiung, Taiwan, 3–7 June 2017; pp. 2218–2222.
3. Saad, A.A.; Faddel, S.; Mohammed, O. A secured distributed control system for future interconnected smart grids. *Appl. Energy* **2019**, *243*, 57–70. [[CrossRef](#)]
4. Heidari-Akhijahani, A.; Safdarian, A.; Lehtonen, M. Unbalance mitigation by optimal placement of static transfer switches in low voltage distribution feeders. *IET Gener. Transm. Distrib.* **2020**, *14*, 4612–4621. [[CrossRef](#)]
5. Shahnia, F.; Wolfs, P.; Ghosh, A. Voltage unbalance reduction in low voltage feeders by dynamic switching of residential customers among three phases. *IEEE Trans. Smart Grid* **2014**, *5*, 1318–1327. [[CrossRef](#)]
6. Amadi, A.K.; Umeogamba, A.I.; Ogbuka, C.U.; Nwosu, C.M.; Chinaeke-Ogbuka, I.M.; Odo, M.C. A 5kva Automatic Transfer Switch with Overload, Short Circuit Protection and Generator Stop Functions. In Proceedings of the 2019 IEEE 1st International Conference on Mechatronics, Automation and Cyber-Physical Computer System, Owerri, Nigeria, 7–8 March 2019; pp. 69–81.
7. Aghaee, F.; Dehkordi, N.M.; Bayati, N.; Hajizadeh, A. Distributed Control Methods and Impact of Communication Failure in AC Microgrids: A Comparative Review. *Electronics* **2019**, *8*, 1265. [[CrossRef](#)]
8. Ortiz, G.; Leibl, M.G.; Huber, J.E.; Kolar, J.W. Design and Experimental Testing of a Resonant DC–DC Converter for Solid-State Transformers. *IEEE Trans. Power Electron.* **2016**, *32*, 7534–7542. [[CrossRef](#)]
9. Alembong, M.A. *Design of a Triac-Based Automatic Transfer Switch (ATS) with Surge Protection*; University of Johannesburg: Johannesburg, South Africa, 2020.
10. Lu, Q.; Zhanqing, Y.; Tianyu, W.; Zhengyu, C.; Bin, L.; Rong, Z. Study on the operating characteristics of a compound automatic transfer switch based on forced current commutation. *J. Eng.* **2019**, *2019*, 3329–3332. [[CrossRef](#)]
11. Gwon, G.-H.; Kim, C.-H.; Oh, Y.-S.; Noh, C.-H.; Jung, T.-H.; Han, J. Mitigation of voltage unbalance by using static load transfer switch in bipolar low voltage DC distribution system. *Int. J. Electr. Power Energy Syst.* **2017**, *90*, 158–167. [[CrossRef](#)]
12. Bertuzzi, G.; Cinti, U.S.; Cevenini, E.; Nalbone, A. Static transfer switch (STS): Application solutions. Correct use of the STS in systems providing maximum power reliability. In Proceedings of the INTELEC 07-29th International Telecommunications Energy Conference, Rome, Italy, 30 September 2007–4 October 2007; pp. 587–594.
13. Javed, M.R.; Mahmood, T.; Choudhry, M.A. Performance analysis of static transfer switch using MATLAB/Simulink. In Proceedings of the 2015 Power Generation System and Renewable Energy Technologies (PGSRET), Islamabad, Pakistan, 10–11 June 2015; pp. 1–5.
14. Roybal, D.D. Transfer switches applied in systems with power circuit breakers. *IEEE Trans. Ind. Appl.* **2001**, *37*, 696–700. [[CrossRef](#)]
15. Roybal, D. Circuit-breaker ratings: Weighing high interrupting capacity and short-time current ratings. *IEEE Ind. Appl. Mag.* **2005**, *11*, 61–71. [[CrossRef](#)]
16. Ransom, D.L. Choosing the Correct Transfer Switch. *IEEE Trans. Ind. Appl.* **2013**, *49*, 2820–2824. [[CrossRef](#)]
17. Yin, J.; Lang, X.; Xu, H.; Duan, J. High-Performance Breaking and Intelligent of Miniature Circuit Breakers. *Sensors* **2022**, *22*, 5990. [[CrossRef](#)] [[PubMed](#)]

18. Gitonga, J.M.; Mwema, W.; Nyete, A.M. Design and Modelling of a Microcontroller Based Automatic Transfer Switch with A Sequential Loading System. In Proceedings of the 2022 IEEE PES/IAS PowerAfrica, Kigali, Rwanda, 22–26 August 2022; pp. 1–5.
19. Wang, G.; Wang, Y.; Zhang, L.; Xue, S.; Dong, E.; Zou, J. A Novel Model of Electromechanical Contactors for Predicting Dynamic Characteristics. *Energies* **2021**, *14*, 7466. [[CrossRef](#)]
20. Usman, A.; Choudhry, M.A. An Efficient and High-Speed Disturbance Detection Algorithm Design with Emphasis on Operation of Static Transfer Switch. *Adv. Electr. Comput. Eng.* **2021**, *21*, 87–98. [[CrossRef](#)]
21. Moschakis, M.N.; Hatziaargyriou, N.D. A detailed model for a thyristor-based static transfer switch. *IEEE Trans. Power Deliv.* **2003**, *18*, 1442–1449. [[CrossRef](#)]
22. Tian, B.; Mao, C.; Lu, J.; Wang, D.; He, Y.; Duan, Y.; Qiu, J. 400 V/1000 kVA Hybrid Automatic Transfer Switch. *IEEE Trans. Ind. Electron.* **2013**, *60*, 5422–5435. [[CrossRef](#)]
23. Hannan, M.A.; Mohamed, A.; Hussain, A. A simulation model of solid-state transfer switch for protection in distribution systems. *J. Appl. Sci.* **2006**, *6*, 1993–1999. [[CrossRef](#)]
24. Mollik, M.S.; Hannan, M.A.; Ker, P.J.; Faisal, M.; Rahman, M.S.A.; Mansur, M.; Lipu, M.S.H. Review on Solid-State Transfer Switch Configurations and Control Methods: Applications, Operations, Issues, and Future Directions. *IEEE Access* **2020**, *8*, 182490–182505. [[CrossRef](#)]
25. Faisal, M.; Hannan, M.A.; Ker, P.J.; Rahman, M.S.; Mollik, M.S.; Mansur, M.B. Review of Solid-State Transfer Switch on Requirements, Standards, Topologies, Control, and Switching Mechanisms: Issues and Challenges. *Electronics* **2020**, *9*, 1396. [[CrossRef](#)]
26. Mahmood, T.; Choudhry, M.A. Performance improvement of complementary feeders using static transfer switch system. *J. Zhejiang Univ. A* **2009**, *10*, 189–200. [[CrossRef](#)]
27. Xu, C.; Zhang, X.; Yu, Z.; Zhao, B.; Chen, Z.; Zeng, R. A Novel DC Chopper With MOV-Based Modular Solid-State Switch and Concentrated Dissipation Resistor for  $\pm 400$  kV/1100 MW offshore Wind VSC-HVDC System. *IEEE Trans. Power Electron.* **2019**, *35*, 4483–4488. [[CrossRef](#)]
28. Hermann, R.; Bernet, S.; Suh, Y.; Steimer, P.K. Parallel Connection of Integrated Gate Commutated Thyristors (IGCTs) and Diodes. *IEEE Trans. Power Electron.* **2009**, *24*, 2159–2170. [[CrossRef](#)]
29. Steimer, P.; Apeldoorn, O.; Carroll, E. IGCT devices-applications and future opportunities. In Proceedings of the 2000 Power Engineering Society Summer Meeting (Cat. No.00CH37134), Seattle, WA, USA, 16–20 July 2000; Volume 2, pp. 1223–1228.
30. Dahlerup-Petersen, K.; Bednarek, M.; Coelingh, G.J.; Dinius, A.; Erokhin, A.; Favre, M.; Siemko, A. A high-current, IGBT-based static switch for energy extraction in superconducting power circuits: Concept, design and production of a 30 kA monopolar and a 1 kA bipolar fast opening switches. In Proceedings of the 2016 IEEE International Power Modulator and High Voltage Conference (IPMHVC), San Francisco, CA, USA, 5–9 July 2016; pp. 508–513.
31. Park, K.-W.; Kim, C.-H. Bi-Directional Power Flow in Switchgear with Static Transfer Switch Applied at Various Renewable Energies. *Energies* **2021**, *14*, 3187. [[CrossRef](#)]
32. Arsad, A.Z.; Sebastian, G.; Hannan, M.A.; Ker, P.J.; Rahman, M.S.A.; Mansur, M.; Lipu, M.S.H. Solid State Switching Control Methods: A Bibliometric Analysis for Future Directions. *Electronics* **2021**, *10*, 1944. [[CrossRef](#)]
33. Shah, K.V. Evolution of Thyristors. *J. Inst. Eng. (India) Ser. B* **2020**, *101*, 553–563. [[CrossRef](#)]
34. Sedaghati, R.; Afrooz, N.M.; Toorani, A.R.; Rohani, A.; Nemati, Y.; Heydarzadegan, A.; Sedaghati, H. Improved power quality solutions using static transfer switch (STS). *Int. Electr. Eng. J. (IEEJ)* **2014**, *5*, 1179–1185.
35. Urciuoli, D.P.; Ibitayo, D.; Koebke, G.; Ovrebø, G.; Green, R. A compact 100-A, 850-V, silicon carbide solid-state DC circuit breaker. In Proceedings of the 2016 IEEE Energy Conversion Congress and Exposition (ECCE), Milwaukee, WI, USA, 18–22 September 2016; pp. 1–5. [[CrossRef](#)]
36. Okilly, A.H.; Baek, J. Design and Fabrication of an Isolated Two-Stage AC–DC Power Supply with a 99.50% PF and ZVS for High-Power Density Industrial Applications. *Electronics* **2022**, *11*, 1898. [[CrossRef](#)]
37. da Silveira, E.P.; Pires, R.C.; de Almeida, A.T.L.; José, A.; Rezek, J. Direct on-line starting induction motor with Thyristor Switched Capacitor based voltage regulation. In Proceedings of the 2009 Brazilian Power Electronics Conference, Bonito, Brazil, 27 September–1 October 2009; pp. 1124–1129.
38. Farazmand, A.; de Leon, F.; Zhang, K.; Jazebi, S. Analysis, Modeling, and Simulation of the Phase-Hop Condition in Transformers: The Largest Inrush Currents. *IEEE Trans. Power Deliv.* **2014**, *29*, 1918–1926. [[CrossRef](#)]
39. Andretto, M.; Pacher, M.; Macii, D.; Palopoli, L.; Fontanelli, D. A distributed strategy for target tracking and rendezvous using UAVs relying on visual information only. *Electronics* **2018**, *7*, 211. [[CrossRef](#)]
40. Okilly, A.H.; Kim, N.; Baek, J. Inrush Current Control of High Power Density DC–DC Converter. *Energies* **2020**, *13*, 4301. [[CrossRef](#)]
41. Ai-Jun, H.; Fei, S.; Wen-Jin, C. Zero-Cross Triggering Technology of Series SCRs with Optical Fiber at Medium Voltage: Application for Thyristor Switched Capacitor. In Proceedings of the 2005 IEEE/PES Transmission & Distribution Conference & Exposition: Asia and Pacific, Dalian, China, 18 August 2005; pp. 1–5.
42. Seo, H.-C.; Gwon, G.-H.; Park, K.-W. New Protection Method Considering Fault Section in LVDC Distribution System with PV System. *J. Electr. Eng. Technol.* **2022**, *18*, 239–248. [[CrossRef](#)]
43. Baek, J. Robust Generator System Using PM Assisted Synchronous Reluctance Generator with Current-Fed Drive. Ph.D. Thesis, Texas A&M University, College Station, TX, USA, 2009.

44. Lin, C.N.; Liao, H.; Chen, J.F.; Lo, C.P. Force Turn-off Method of SCR for UPS. In Proceedings of the 2021 IEEE International Future Energy Electronics Conference (IFEEEC), Taipei, Taiwan, 16 November 2021; pp. 1–8.
45. Mokhtari, H.; Dewan, S.B.; Iravani, M.R. Analysis of a static transfer switch with respect to transfer time. *IEEE Trans. Power Deliv.* **2002**, *17*, 190–199. [[CrossRef](#)]
46. Cheng, P.-T.; Tsai, C.-H. An improved solid-state transfer switch controller for sensitive industrial loads. In Proceedings of the 2003 IEEE Power Engineering Society General Meeting (IEEE Cat. No. 03CH37491), Toronto, ON, Canada, 13–17 July 2003; Volume 4, pp. 2514–2519.
47. Wu, J.; Xu, J.; Lv, D. Optimal design of the mechanical switch suitable for the ATS. *J. Eng.* **2019**, *2019*, 2589–2592. [[CrossRef](#)]
48. Amuzuvi, C.K.; Addo, E. A microcontroller-based automatic transfer switching system for a standby electric generator. *Ghana Min. J.* **2015**, *15*, 85–92.

**Disclaimer/Publisher’s Note:** The statements, opinions and data contained in all publications are solely those of the individual author(s) and contributor(s) and not of MDPI and/or the editor(s). MDPI and/or the editor(s) disclaim responsibility for any injury to people or property resulting from any ideas, methods, instructions or products referred to in the content.